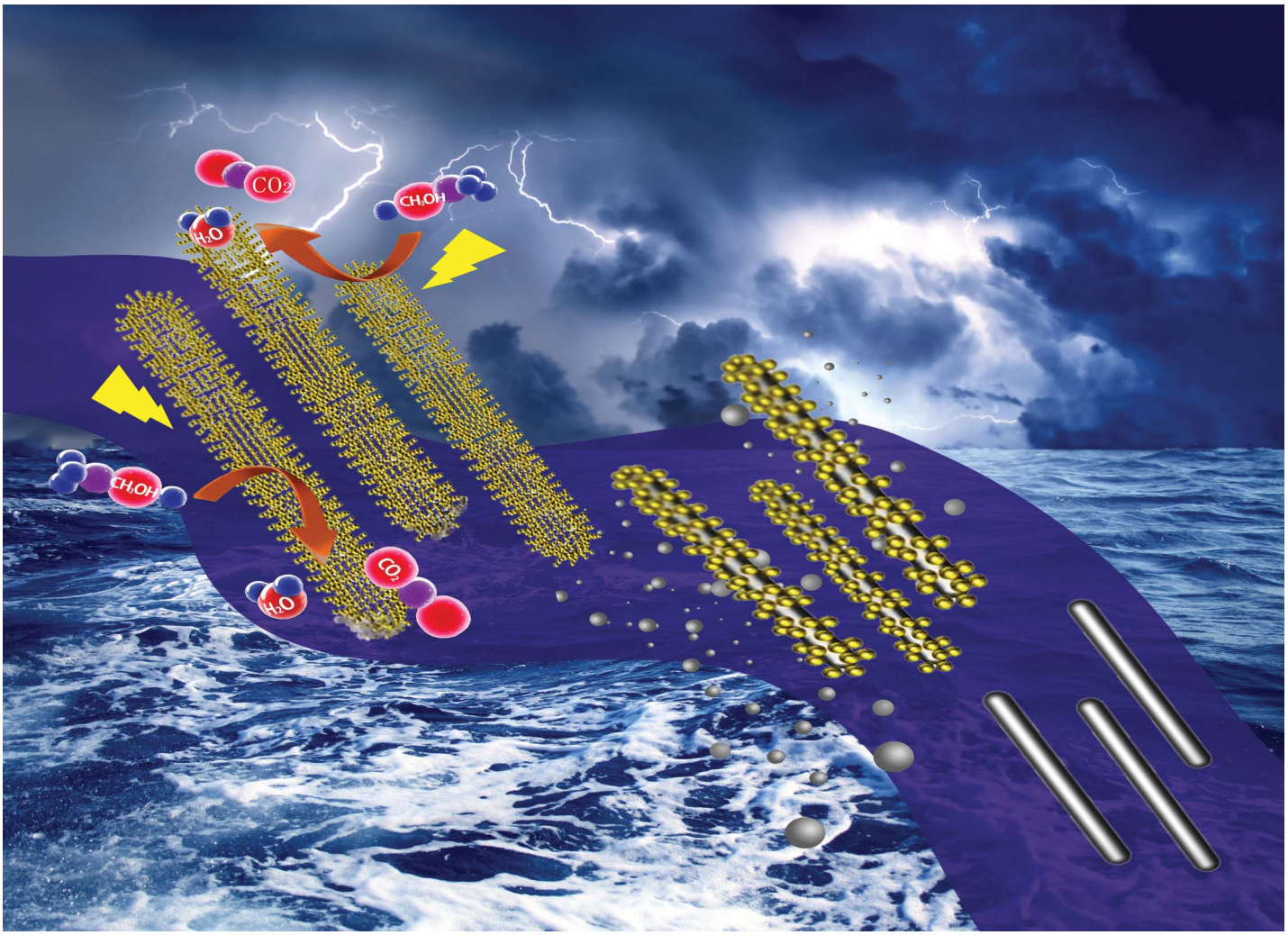

Showcasing research from Heyou Han's Research Laboratory (Nano-Bioanalytic Laboratory), State Key Laboratory of Agricultural Microbiology, College of Science, Huazhong Agricultural University, China.

Title: Spiny-porous platinum nanotubes with enhanced electrocatalytic activity for methanol oxidation

A facile and general approach is developed to synthesize self-supported spiny-porous Pt nanotubes (SP-PtNTs) with high aspect ratio and enriched edge and corner atoms. The as-prepared SP-PtNTs exhibited significantly enhanced activity and stability to methanol electro-oxidation in an acid medium, demonstrating the potential application of SP-PtNTs as effective electrocatalysts for DAFCs.

As featured in:

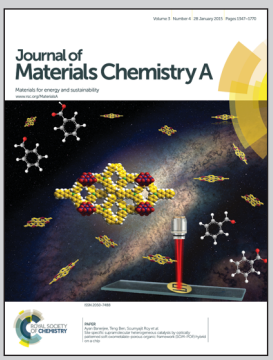

See Heyou Han *et al.*, *J. Mater. Chem. A*, 2015, **3**, 1388.

ROYAL SOCIETY OF CHEMISTRY

www.rsc.org/MaterialsA

Registered charity number: 207890

Journal of Materials Chemistry A

COMMUNICATION

View Article Online
View Journal | View Issue

Cite this: J. Mater. Chem. A, 2015, 3, 1388

Received 12th October 2014
Accepted 22nd November 2014

DOI: 10.1039/c4ta05443a

www.rsc.org/MaterialsA

Spiny-porous platinum nanotubes with enhanced electrocatalytic activity for methanol oxidation†

Yunpeng Zuo, Kai Cai, Long Wu, Tingting Li, Zhicheng Lv, Jiawei Liu, Kang Shao and Heyou Han*

A facile and general approach is developed to synthesize self-supported spiny-porous Pt nanotubes (SP-PtNTs). The multi-dimensional structure with enriched edge and corner atoms showed 4.3 and 1.53 times higher mass electrocatalytic activity than porous Pt nanotubes (P-PtNTs) and commercial Pt/C (20% Pt), which increased the Pt utilization and decreased the dosage of Pt and the cost of Pt-based catalysts. SP-PtNTs had better stability and dispersibility than P-PtNTs and commercial Pt/C (20% Pt) in the water phase. The brief mechanism for the synthesis of SP-PtNTs could also be extended to synthesize other noble metals, as well as their bimetallic combinations, with excellent catalysis and electrocatalysis. Furthermore, the spiny structure provided extra active sites that might facilitate the application of Pt for use in enzyme-like catalysis or nano-electronic applications.

As a catalyst, platinum has extensive applications in many areas such as direct methanol fuel cells (DMFCs) and the mobile terminals industry.[1] However, the high cost of Pt catalysts and the limited Pt reserves are obstacles that severely limits their application.[2] Therefore, it is urgent to produce Pt catalysts with a large surface area to achieve high catalytic performance and utilization efficiency.[3] Previous reports have focused on decreasing the Pt loading and boosting the Pt utilization while maintaining satisfactory activity and stability,[3,4] which could be an alternative to synthesizing shape-controlled Pt nanomaterials with a large number of edges and corners atoms, which can actually enhance the catalytic activity owing to the valency unsaturated atoms.[5] The Pt-based electrocatalysts are active when the fractal dimensionality is in the range of nanoscale. However, the Pt-based catalysts could easily aggregate because of the large surface energy, which would obviously decrease the catalytic activity.[2c,6] Hence, it is important to seek approaches for the synthesis of self-supported Pt-based catalysts with enriched edge and corner atoms to enhance the catalytic performance and efficient utilization of Pt materials.

A reasonable expectation would be that the Pt catalysts were synthesized using one-dimensional (1D) nanomaterials as a template, which has been demonstrated as a practical method for the synthesis of morphology-controlled Pt nano-materials.[7] Compared with zero-dimensional (0D) Pt, 1D nanostructures have attracted extensive attention due to their improved catalytic and electronic properties.[1a,8] Synthesis of 1D Pt nanomaterials can use various types of templates, such as carbon nanotubes,[9a] polymer nanotubes,[9b–d] and tellurium nanowires.[9e] Compared with carbon nanotubes, tellurium nanowires and polymer nanotubes can be chemically synthesized in bulk without sophisticated instruments or sophisticated technology.[9d,e] Carbon or polymer nanotubes can be used as supports to enhance the stability of Pt nanomaterials while it is hard to control the morphology of the metal. TeNWs could be easily removed, which might be conducive to synthesize new morphology of self-supported Pt nanomaterials. Inspired by this, it is facile and efficient to synthesize P-PtNTs with a large surface area using TeNWs as a template, and the unique structure may further promote their catalytic activity.[1b,9e] Based on the P-PtNTs, the spiny structure grown on their surface would further increase the surface area and the ratio of the edges and corners atoms, thereby enhancing the catalytic activity of the P-PtNTs for methanol electro-oxidation.[1c,5a,b,10]

In this paper, we developed a facile method to synthesize SP-PtNTs with well-defined morphologies as illustrated in Scheme 1. The synthetic process was in the water phase conditions using TeNWs as sacrificial templates, chloroplatinic acid as a platinum source and cetyltrimethylammonium bromide (CTAB) as the surfactant. In the synthesis of SP-PtNTs, the as-prepared TeNWs (Fig. S1†) were first added to the solution of cetyltrimethylammonium bromide (CTAB), and then an aqueous solution of H_2PtCl_6 (pH = 7) was injected. Detailed experimental procedures were presented in ESI.† Finally, the resultant mixture was heated to around 30 °C for about 30 min to obtain the SP-PtNTs.

State Key Laboratory of Agricultural Microbiology, College of Science, Huazhong Agricultural University, Wuhan 430070, P. R. China. E-mail: hyhan@mail.hzau.edu.cn

† Electronic supplementary information (ESI) available. See DOI: 10.1039/c4ta05443a

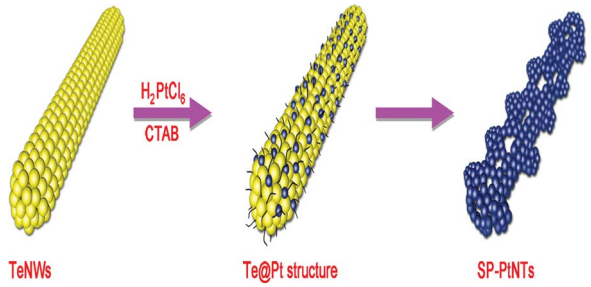

Scheme 1 Schematic illustration of the evolution from TeNWs to SP-PtNTs with well-defined morphologies.

The X-ray diffraction (XRD) pattern of SP-PtNTs in Fig. S2† shows that all peaks can be indexed to face-centered cubic (fcc) platinum with a lattice constant of $a = 0.39$ nm, which is consistent with the standard literature values (JCPDS no.04-0802) and also indicates that TeNWs have been effectively transferred to SP-PtNTs.[10a] The energy-dispersive X-ray (EDX) spectra of the SP-PtNTs (Fig. S3†) shows the peaks were in accordance with Pt elements, which further confirms the above conclusions. As depicted in Fig. 1, the TEM images of SP-PtNTs derived from the TeNWs under different magnifications show an excellent structure with an average diameter of ~22 nm with a narrow diameter distribution. On the basis of the high resolution TEM (HRTEM) shown in Fig. 1D, it is clear that the PtNts are provided with spiny and porous structures, and the *d*-spacing of adjacent fringes for the spiny structure is 0.23 nm, which corresponds to the (111) planes of a face-centered cubic (fcc) Pt. The highly crystalline spiny Pt structure consisting of large edges and corner atoms are favorable for enhancing the catalytic performance and reducing the costs of fuel cells.[10b]

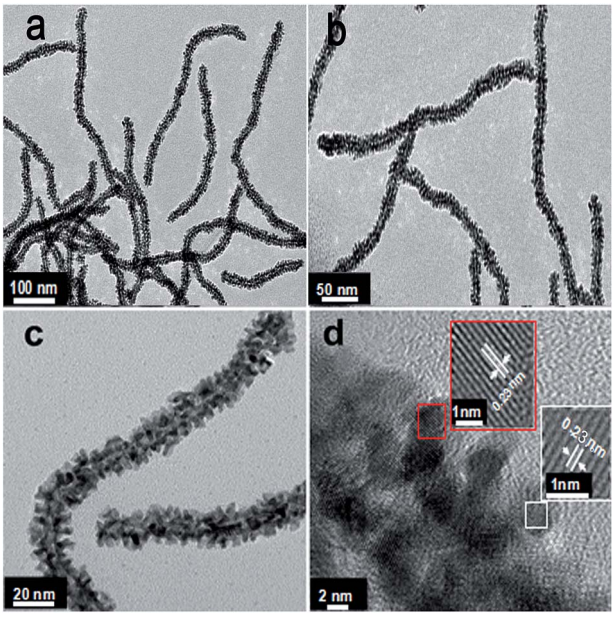

Fig. 1 (a) TEM image of the SP-PtNTs used TeNWs as templates. (b and c) Magnified TEM images of the special Pt. (d) HRTEM and filtered image of the square area.

The CTAB plays an important role in the formation of the SP-PtNTs based on TeNWs. Only Pt nanowires were obtained without the addition of CTAB (Fig. S4a†), whereas as the concentration of CTAB increased to 16 mM, the final products would be the mixture of Pt nanodendrites and SP-PtNTs (Fig. S4b†). By further increasing the concentration of CTAB to 30 mM, pure SP-PtNTs were obtained (Fig. S4c†). This result reveals that the SP-PtNTs are generated only with a suitable concentration of CTAB. Here, the use of CTAB as a surfactant to control the reaction kinetics might have four advantages: (1) Pt nanocrystals would grow along the ⟨111⟩ direction in the presence of CTAB, which might play a key role in the formation of special structure;[4c] (2) the hydrophilic group CTA^+ of the CTAB colloid solution with amino-group is positively charged, which could enrich $PtCl_6^{2-}$ around the TeNWs;[11] (3) the concentration of CTAB is larger than its cmc value at 30 °C and the distribution of CTAB might be conducive to the synthesis of SP-PtNTs;[12] (4) CTAB might have a good compatible effect with other zwitterionic surfactants, which is very important to the repeatable synthesis of SP-PtNTs.[13] Fig. 2 describes the major steps involved in the synthesis of SP-PtNTs. The galvanic replacement would occur immediately at the site with the highest surface energy when an aqueous H_2PtCl_6 (pH = 7) solution is added into the suspension of the as-prepared TeNWs.[14] CTA^+ might strongly interact with $PtCl_6^{2-}$ in the aqueous solution resulting in the complexation of CTA^+–$PtCl_6^{2-}$, which could enrich $PtCl_6^{2-}$ around the TeNWs.[15a] Te atoms will be oxidized into TeO_3^{2-} by the $PtCl_6^{2-}$ and dissolved into the solution. At the same time, $PtCl_6^{2-}$ will quickly capture the electrons from Te → TeO_3^{2-} and equivalent molar amounts of Pt could be generated when Te atoms are oxidized into TeO_3^{2-}; however, the molar volume of Te is larger than that of Pt, thus resulting in the formation of holes on the surface of the nanowires.[10b] The newly formed Pt atoms on the surface of TeNWs would be deposited epitaxially in the presence of CTAB (step 1 in Fig. 2).[15b] As the reaction proceeds, a thin and incomplete layer of Pt would be generated on the surface of TeNWs and the unreacted Te will be

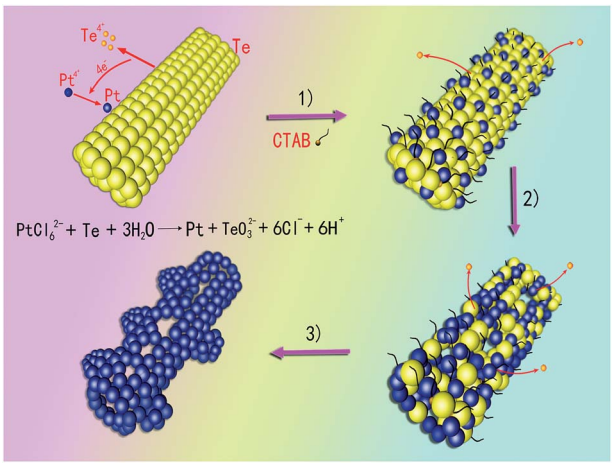

Fig. 2 Schematic illustration of the morphological changes at different stages of the galvanic replacement reaction between TeNWs and H_2PtCl_6 in an aqueous solution.

limited to react with $PtCl_6^{2-}$.[14c] Then, the Te atoms in the layer of Pt would be dissolved and form the cavity, which can serve as the primary site for continuous dissolution of Te, while the $PtCl_6^{2-}$ could be reduced by Te (step 2 in Fig. 2).[14c,16] As the reaction continues, Te atoms from the template would be completely dissolved, which transforms the nanowire structure into SP-PtNTs (step 3 in Fig. 2).

Based on high-energy density liquid fuels, low-temperature fuel cells as power sources have attracted considerable attention. Methanol is one of the major renewable biofuels and direct alcohol fuel cells (DAFCs), which can improve reaction kinetics and be less corrosive to the electrodes.[1b] Recent studies have revealed that Pt nanostructures enriched with edges and corners atoms are highly favorable for methanol electrochemical oxidation in acidic media, indicating the potential application to DMFCs.[3,17] Therefore, SP-PtNTs are supposed to be advanced functional materials in fuel cells. To observe the electro-catalytic activity and stability of the Pt material, the properties of the self-supported SP-PtNTs, P-PtNTs and Pt/C (20% Pt) were evaluated. First, the cyclic voltammetry (CV) curves of three catalysts were tested at room temperature in 0.5 M H_2SO_4 solution at a sweep rate of 50 mV s^{-1}. Fig. 3a shows the characteristic peaks for the Hupd ($H^+ + e^- = Hupd$) adsorption/desorption in the potential region from −0.2 to 0.1 V and reduction of Pt oxide for the OHad ($2H_2O = OHad + H_3O^+ + e^-$) between 0.4 and 1.2 V. Thus, Q_H and the integrated area of the adsorption peak in the CV curves were obtained and were used to calculate the electro-chemical surface area (ECSA) of SP-PtNTs, P-PtNTs, and Pt/C (20% Pt).[18] The specific ECSAs (the ECSA per g_{Pt}) of SP-PtNTs, P-PtNTs, and Pt/C (20% Pt) were 46.5, 23.3 and 68.7 $m^2\ g_{Pt}^{-1}$. Elemental content was measured by inductively coupled plasma-atomic emission spectrometry (ICP-AES). The ECSA of SP-PtNTs is two times higher than that of P-PtNTs, which was lower than that of Pt/C (20% Pt) (68.7 $m^2\ g_{Pt}^{-1}$). The results show that the spiny structure can effectively increase the ECSA of the material, as shown in Fig. 3b. The lower ECSA of the SP-PtNTs and P-PtNTs catalysts were mainly attributed to the large size of the Pt structure compared with that of Pt nanoparticles (about 3 nm) in commercial catalysts.[4c]

In addition, the electrocatalytic performance of the SP-PtNTs for the methanol oxidation reaction (MOR) was achieved as shown in Fig. 3. Particularly, Fig. 3c displays the CV curves of the MOR for the three catalysts in 0.5 M H_2SO_4 + 1 M CH_3OH solution at a scan rate of 50 mV s^{-1}, and the GC electrode coated with the SP-PtNTs exhibited a peak current density (0.26 mA μg^{-1}), which is higher than P-PtNTs (0.06 mA μg^{-1}) and Pt/C (20% Pt) (0.17 mA μg^{-1}), which is shown in Fig. 3d. The significantly higher methanol oxidation results of the two well-defined current peaks for the SP-PtNTs, one on the forward and the other on the reverse potential scans, clearly demonstrating a higher mass activity mainly due to the higher utilization of large surface area and high ratio of the edges and corner atoms on the spiny structure, which is in accordance with the results of the specific activity for the three catalysts (0.55 mA cm^{-2}), (0.26 mA cm^{-2}) and (0.17 mA cm^{-2}), respectively. Chronoamperometry was employed to further investigate the electrochemical performance of the three catalysts and the results are shown in Fig. 3e. Potential-dependent steady-state current (recorded at 1000 s) of methanol electro-oxidation for the three catalysts was also investigated and is shown in Fig. 3f. The results reveal that the SP-PtNTs have better performance for methanol electro-oxidation than the P-PtNTs or commercial Pt/C (20% Pt) catalysts for all applied potentials, which demonstrates that a spiny structure full of edges and corner atoms can effectively enhance the inherent catalytic activity of the material.

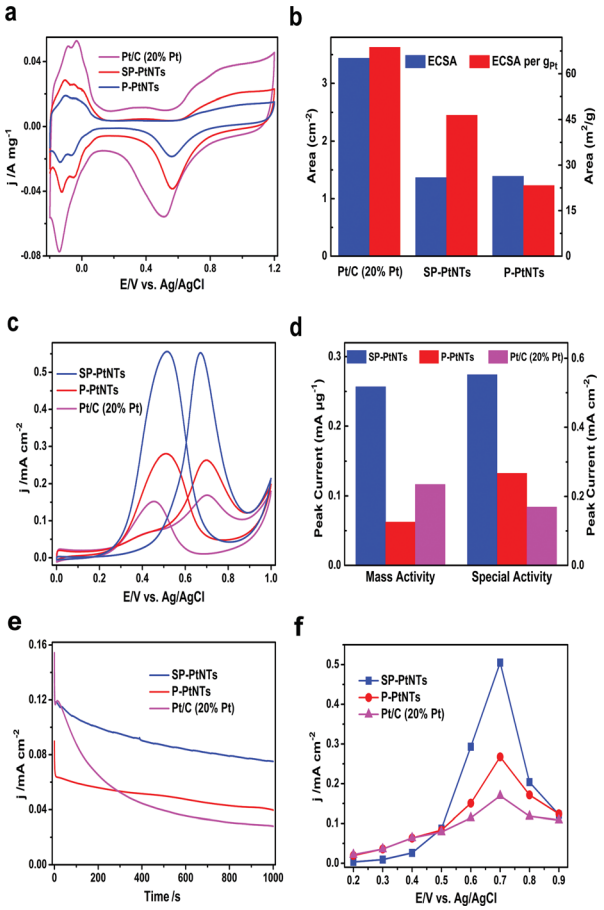

Fig. 3 (a) CV curves for the SP-PtNTs, P-PtNTs, and Pt/C (20% Pt) in 0.5 M H_2SO_4 solution at 50 mV s^{-1}. (b) ECSA and ECSA per g_{Pt} for three catalysts. (c) Methanol oxidation reaction catalyzed by the three catalysts in 0.5 M H_2SO_4 + 1 M CH_3OH solution at 50 mV s^{-1}. (d) Mass activity and specific activity of the three catalysts. (e) Current density–time curves of the three catalysts in 0.5 M H_2SO_4 + 1 M CH_3OH solution at 0.5 V. (f) Potential-dependent steady-state current (recorded at 1000 s) of methanol electro-oxidation for the three catalysts. The loading amounts of Pt are 41.6, 84.4 and 70.8 μg cm^{-2} for SP-PtNTs, P-PtNTs, and Pt/C (20% Pt) catalyst, respectively.

In conclusion, we have developed a facile and general approach to synthesize SP-PtNTs structured with a high aspect ratio and an enriched population of edges and corners atoms. The as-prepared SP-PtNTs exhibited significantly enhanced activity and stability towards methanol electro-oxidation in an acidic medium, demonstrating the potential application of SP-PtNTs as effective electrocatalysts for DAFCs. Further studies revealed that CTAB played an important role in the synthesis of the well-defined spiny nanostructures. Moreover, the new

strategy for the synthesis of SP-PtNTs could also be extended to synthesize other noble metals as well as their bimetallic combinations with excellent catalysis and electrocatalysis properties.

Acknowledgements

This work was supported by the National Natural Science Foundation of China (21375043, 21175051).

Notes and references

1 (*a*) B.-Y. Xia, H.-B. Wu, Y. Yan, X.-W. Lou and X. Wang, *J. Am. Chem. Soc.*, 2013, **135**, 9480; (*b*) S.-M. Alia, G. Zhang, D. Kisailus, D. Li, S. Gu, K. Jensen and Y. Yan, *Adv. Funct. Mater.*, 2010, **20**, 3742; (*c*) S. Guo, S. Dong and E. Wang, *Chem. Commun.*, 2010, **46**, 1869; (*d*) Z. Huang, H. Zhou, F. Sun, C. Fu, F. Zeng, T. Li and Y. Kuang, *Chem.–Eur. J.*, 2013, **19**, 13720.

2 (*a*) H.-P. Liang, H.-M. Zhang, J.-S. Hu, Y.-G. Guo, L.-J. Wan and C.-L. Bai, *Angew. Chem., Int. Ed.*, 2004, **43**, 1540; (*b*) H.-H. Li, S. Zhao, M. Gong, C.-H. Cui, D. He, H.-W. Liang, L. Wu and S.-H. Yu, *Angew. Chem., Int. Ed.*, 2013, **52**, 7472; (*c*) D. Zhao and B.-Q. Xu, *Angew. Chem., Int. Ed.*, 2006, **45**, 4955.

3 R.-A. Martinez-Rodriguez, F.-J. Vidal-Iglesias, J. Solla-Gullon, C.-R. Cabrera and J.-M. Feliu, *J. Am. Chem. Soc.*, 2014, **136**, 1280.

4 (*a*) B. Genorio, D. Strmcnik, R. Subbaraman, D. Tripkovic, G. Karapetrov, V.-R. Stamenkovic, S. Pejovnik and N.-M. Marković, *Nat. Mater.*, 2010, **9**, 998; (*b*) B. Lim and Y. Xia, *Angew. Chem., Int. Ed.*, 2011, **50**, 76; (*c*) B.-Y. Xia, H.-B. Wu, X. Wang and X.-W. Lou, *Angew. Chem., Int. Ed.*, 2013, **52**, 12337; (*d*) D. Xu, S. Bliznakov, Z. Liu, J. Fang and N. Dimitrov, *Angew. Chem., Int. Ed.*, 2010, **49**, 1282; (*e*) X. Luo and S. Yang, *Nanoscale*, 2014, **6**, 4438.

5 (*a*) L. Wang and Y. Yamauchi, *J. Am. Chem. Soc.*, 2009, **131**, 9152; (*b*) L. Wang, H. Wang, Y. Nemoto and Y. Yamauchi, *Chem. Mater.*, 2010, **22**, 2835; (*c*) C.-E.-T.-M. A. Mahmoud, M. A. El-Sayed, Y. Ding and Z.-L. Wang, *J. Am. Chem. Soc.*, 2008, **130**, 4590–4591.

6 (*a*) Z. Peng and H. Yang, *Nano Today*, 2009, **4**, 143; (*b*) H. Zhang, M. Jin and Y. Xia, *Angew. Chem., Int. Ed.*, 2012, **51**, 7656.

7 (*a*) Y. Liu, J. Goebl and Y. Yin, *Chem. Soc. Rev.*, 2013, **42**, 2610; (*b*) Y. Xia, Y. Xiong, B. Lim and S.-E. Skrabalak, *Angew. Chem., Int. Ed.*, 2009, **48**, 60–103; (*c*) L. Cademartiri and G.-A. Ozin, *Adv. Mater.*, 2009, **21**, 1013–1020.

8 Y.-J. Song, R.-M. Garcia, R.-M. Dorin, H.-R. Wang, Y. Qiu, E.-N. Coker, W.-A. Steen, J.-E. Miller and J.-A. Shelnutt, *Nano Lett.*, 2007, **7**, 3650.

9 (*a*) S.-I. Cho and S.-B. Lee, *Acc. Chem. Res.*, 2008, **41**, 699; (*b*) X. Wu, L.-H. Qiu, Z.-Z. Yang and F. Yan, *Appl. Catal., A*, 2014, **478**, 30–37; (*c*) Y.-J. Peng, L.-H. Qiu, C.-T. Pan, C.-C. Wang, S.-M. Shang and F. Yan, *Electrochim. Acta*, 2012, **75**, 399–405; (*d*) L.-H. Qiu, B.-Q. Liu, Y.-J. Peng and F. Yan, *Chem. Commun.*, 2011, **47**, 2934–2936; (*e*) X. Zhang, W. Lu, J. Da, H. Wang, D. Zhao and P.-A. Webley, *Chem. Commun.*, 2009, 195–197.

10 (*a*) H.-W. Liang, S. Liu, J.-Y. Gong, S.-B. Wang, L. Wang and S.-H. Yu, *Adv. Mater.*, 2009, **21**, 1850; (*b*) A.-K. Prashar, R.-P. Hodgkins, J.-N. Chandran, P.-R. Rajamohanan and R.-N. Devi, *Chem. Mater.*, 2010, **22**, 1633.

11 C. Jeyabharathi, S.-S. Kumar, G.-V. Kiruthika and K.-L. Phani, *Angew. Chem.*, 2010, **49**, 2925.

12 Y. Kim, J.-W. Hong, Y.-W. Lee, M. Kim, D. Kim, W.-S. Yun and S.-W. Han, *Angew. Chem., Int. Ed.*, 2010, **49**, 10197.

13 S.-Y. Shiao, V. Chhabra, A. Patist, M.-L. Free, P.-D.-T. Huibers, A. Gregory, S. Patel and D.-O. Shah, *Adv. Colloid Interface Sci.*, 1998, **74**, 1–29.

14 (*a*) X. Hong, D. Wang, S. Cai, H. Rong and Y. Li, *J. Am. Chem. Soc.*, 2012, **134**, 18165; (*b*) Z.-L. Wang, *J. Phys. Chem. B*, 2000, **104**, 1153; (*c*) X. Xia, Y. Wang, A. Ruditskiy and Y. Xia, *Adv. Mater.*, 2013, **25**, 6313.

15 (*a*) A. Takai, Y. Yamauchi and K. Kuroda, *J. Mater. Chem.*, 2009, **19**, 4205–4210; (*b*) B.-Y. Xia, H.-B. Wu, X. Wang and X.-W. (David) Lou, *Angew. Chem., Int. Ed.*, 2012, **51**, 7213.

16 (*a*) Y. Sun and Y. Xia, *J. Am. Chem. Soc.*, 2004, **126**, 3892; (*b*) N.-P. Dasgupta, J. Sun, C. Liu, S. Brittman, S.-C. Andrews, J. Lim, H. Gao, R. Yan and P. Yang, *Adv. Mater.*, 2014, **26**, 2137.

17 (*a*) S. Guo, S. Dong and E. Wang, *ACS Nano*, 2010, **4**, 547; (*b*) B. Lim and Y. Xia, *Angew. Chem., Int. Ed.*, 2011, **50**, 76–85.

18 H. You, F. Zhang, Z. Liu and J. Fang, *ACS Catal.*, 2014, **4**, 2829–2834.